JOURNAL OF OPTOELECTRONICS AND ADVANCED MATERIALS, Vol. 11, No. 6, June 2009, p. 863 - 869

Laser-induced damage threshold at different wavelengths of Ta_2O_5 films of wide-range temperature annealing

CHENG XU[a*], YINGHUAI QIANG[a], YABO ZHU [a], JIANDA SHAO[b], ZHENGXIU FAN[b]
[a]*School of Materials Science and Engineering, China University of Mining and Technology, Jiangsu 221116, China*
[b]*Shanghai Institute of Optics and Fine Mechanics, Chinese Academy of Sciences, Shanghai 201800, China*

The laser-induced damage of Ta_2O_5 films annealed at wide-range temperature (473-1273 K) at the laser wavelengths of 1064 nm and 355 nm was investigated. The relations among microstructure, optical properties, absorption, chemical composition and laser-induced damage threshold (LIDT) at different wavelengths were researched. The dependence of damage mechanism on laser wavelength was discussed. It was found that both the LIDT increases firstly and then decreases with the increase of annealing temperature either at 1064 nm or 355 nm. The LIDT at 1064 nm was influenced mainly by the substoichiometric defect, structural defect and thermal diffusion, whereas at 355 nm it was influenced more significantly by the intrinsic absorption and structural defect. Both the maximum LIDT at the two wavelengths was achieved at the annealing temperature of 873 K, which could be attributed to the lowest defect density in the films.

(Received May 17, 2009; accepted June 15, 2009)

Keywords: Ta_2O_5 films, Annealing, Laser-induced damage threshold, Absorption

1. Introduction

Ta_2O_5 is one of the most important materials for optical coatings as it has wide transparent spectra, high refractive index and strong adhesion to substrates. However, it is a disadvantage that Ta_2O_5 films are liable to be substoichiometry in the electron beam evaporation deposition process, so annealing is always performed for achieving better stoichiometry [1,2]. The laser-induced damage of optical films is a key issue in the research of high-power laser systems. The damage mechanism has not been fully understood as it is complicated and associated with many factors [3,4]. For Ta_2O_5 single and multiple films, the laser-induced damage threshold (LIDT) at 1064 nm has been extensively investigated, which indicates that the damage is correlated with substrates, protective layers, laser characteristics and post-annealing [5-10]. The damage at 1064 nm has always been observed with defects, and the LIDT can be improved by decreasing the density or enhancing the stability of defects [11,12]. The wavelength dependence of damage of Ta_2O_5 films has been reported at 1064, 800 and 532 nm [13]. When the wavelength decreases to 355 nm, the intrinsic absorption of Ta_2O_5 material would be considered to contribute to the damage initiation.

In this paper, wide-range temperature (473-1273 K) annealing treatment was performed on Ta_2O_5 films deposited by electron beam evaporation. The main aim was to investigate the correlations of the LIDT at different wavelengths with the microstructure, optical properties, chemical composition and absorption of varied annealing Ta_2O_5 films. The detailed damage mechanism at different wavelengths was discussed.

2. Experimental

Ta_2O_5 films were deposited on fused silica substrates by electron beam evaporation. The base pressure was 2×10^{-3} Pa and oxygen partial pressure was 2×10^{-2} Pa during deposition. The substrate temperature was kept at 573 K during deposition. The films were annealed in air at 473, 673, 873, 1073 and 1273 K for 8 h after annealing, respectively. LIDT at 1064 nm (12 ns) and 355 nm (8 ns) were tested in the 1-on-1 regime with the ISO standard 11254-1 [14]. Microstructure of Ta_2O_5 films was analyzed by X-ray diffractometer. Transmittance spectra of films were measured with a Perkin-Elmer Lambda 900 spectrophotometer. The optical constants were obtained by photometric method from the measured transmittance spectral curves [15]. The film thickness was measured with WYKO NT1100 profilometer. Surface topography was observed by Nanocope atomic force microscope (AFM). The composition of films was analysed by X-ray photoelectron spectroscopy (XPS) (Thermo ESCALAB 250). The absorption of films was measured by surface thermal lensing method, and the pump source used in the experimental setup is a single-mode, CW YAG 1064 nm

laser [16,17]. The damage morphologies were observed by a Leica-DMRXE microscope.

3. Results

Fig. 1 shows the LIDT results at different wavelengths of films. It is illustrated in Fig. 1(a) that the LIDT at 1064 nm increases firstly and then decreases with the increase of annealing temperature. Moreover, all the annealed films have higher LIDT than the as-deposited film. When the annealing temperature is 873 K the highest LIDT of 11.7 J/cm^2 obtains, increasing by about 160% than that of the as-deposited film (4.5 J/cm^2). Fig. 1(b) shows that the LIDT at 355 nm is much lower than that at 1064 nm. In addition, similar tendency is observed in Fig. 1(b) as in Fig. 1(a) that the LIDT increases firstly and then decreases above 873 K. The maximum LIDT at 355 nm also achieves at 873 K, which is 1.9 J/cm^2, only increasing by about 36% than the as-deposited film (1.5 J/cm^2). Furthermore, Fig. 1(b) shows that the LIDT of films annealed at 1073 and 1273 K is 1.3 J/cm^2 and 0.7 J/cm^2, respectively, which is lower than the as-deposited film.

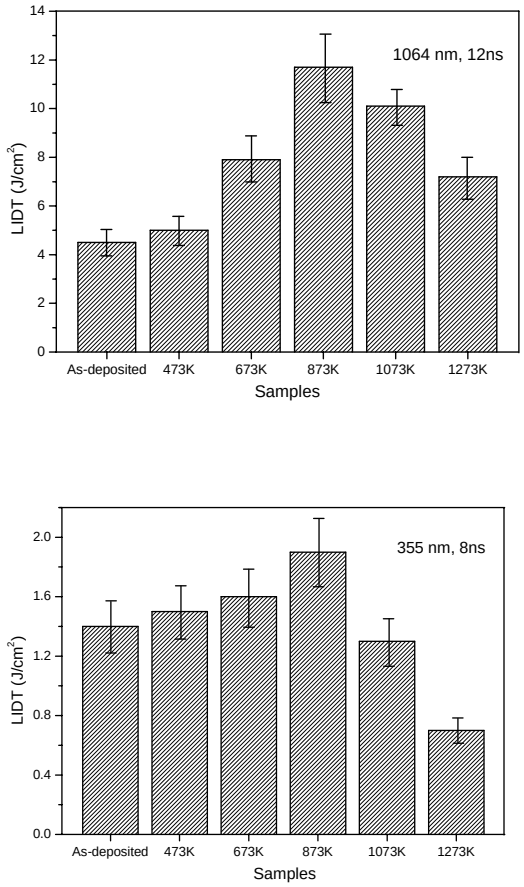

Fig. 1. The LIDT at 1064 nm, 12 ns (a) and 355 nm, 8 ns (b) of films.

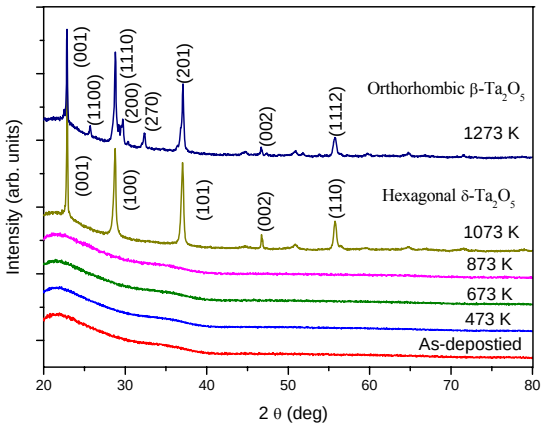

Fig. 2. XRD patterns of films.

XRD patterns of Ta_2O_5 films annealed at different temperature are illustrated in Fig. 2. It shows that the films are amorphous when the annealing temperature is lower than 1073 K. As the temperature increases to 1073 K, XRD analysis reveals the preferred formation of hexagonal δ-Ta_2O_5 phase (Card 19-1299) [18]. The film becomes strongly crystallized showing the most intense (001), (100) and (101) diffractions at 2θ=23.2, 28.5 and 36.9°, respectively. In addition, the (002) and (110) diffractions with lower intensity appear at 47.0 and 50.5°, respectively. The film annealed at 1273 K exhibits two distinct XRD diffraction peaks at 28.4 and 28.7°, which can be associated with the (1110) and (200) diffraction of orthorhombic β-Ta_2O_5 phase (Card 25-0922) [18,19]. The average grain sizes of films are calculated by Scherrer's equation shown in Table 1. It demonstrates that the grain sizes of films annealed at 1073 and 1273 K are 62 and 82 nm, respectively.

Table 1. The average grain sizes of films.

Annealing temperature (K)	2θ (°)	β (°)	D (nm)
As-deposited-873	-	-	-
1073	22.8669	0.1301	62
1273	22.8425	0.0973	82

Fig. 3(a) shows that the optical transmittance increases firstly upon increasing annealing temperature

especially in the short wavelength region. When the annealing temperature increases to 1073 K, the transmittance spectra start to decrease.

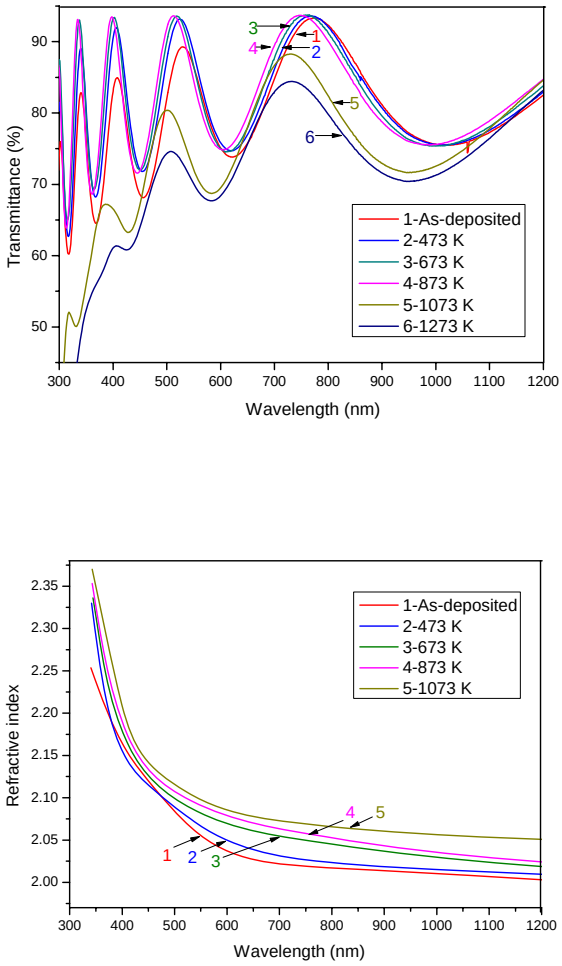

Fig. 3. Transmittance spectra (a) and refractive index (b) of films.

The refractive index of films is shown in Fig. 3(b), however, it is difficult to extract the refractive index accurately for the film annealed at 1273 K. It is illustrated that the refractive index increases with the annealing temperature increasing.

The refractive index is a function of the film's density. As is shown in Fig. 3(b), the as-deposited film is looser. During annealing, thermal energy provides the mobility of the atoms, so the loose columns in the as-deposited film become densified as the temperature increases, which also increases the refractive index. The film thickness measured by profilometer is shown in Fig. 4. It decreases with the increase of annealing temperature, confirming that the film's density increases during annealing.

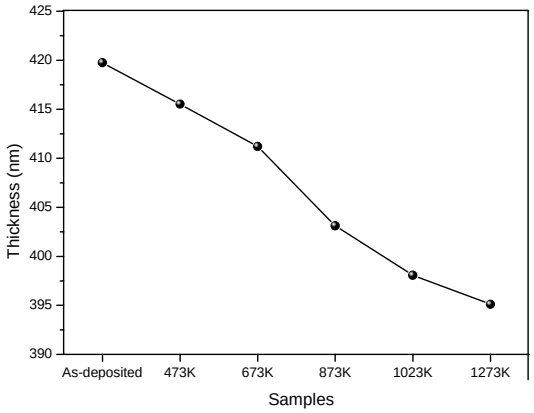

Fig. 4. Physical thickness of films.

The evolution of surface topography of films is shown in Fig. 5. The root mean square (RMS) roughness slightly increases when the annealing temperature is no higher than 873 K, which is 5.831 , 6.215, 8.102 and 9.364 nm. However, the RMS roughness increases significantly to 31.367 and 43.699 nm when the annealing temperature increases to 1073 and 1273 K, respectively, which can be attributed to the crystallization of Ta_2O_5 films. In addition, as crystal grows up rapidly in the phase transition process, some microcracks can be observed on the surface of the film annealed at 1273 K. Figure 6 displays the Ta 4f spectra of films. The spectra reveal two $4f_{7/2}$ and $4f_{5/2}$ peaks at 26.4 and 28.2 eV, which shows the composition of films is Ta^{5+} [20]. The O/Ta ratio is estimated from the XPS peak areas together with their relative sensitivity factors. The O/Ta ratio of the as-deposited film is 2.42. When annealed at 473 K, it increases to 2.44. After annealed above 673 K, all the O/Ta ratio increases to 2.50. It is concluded that during the annealing course, oxygen penetrates and reacts with the substoichiometry films, improving the stoichiometry.

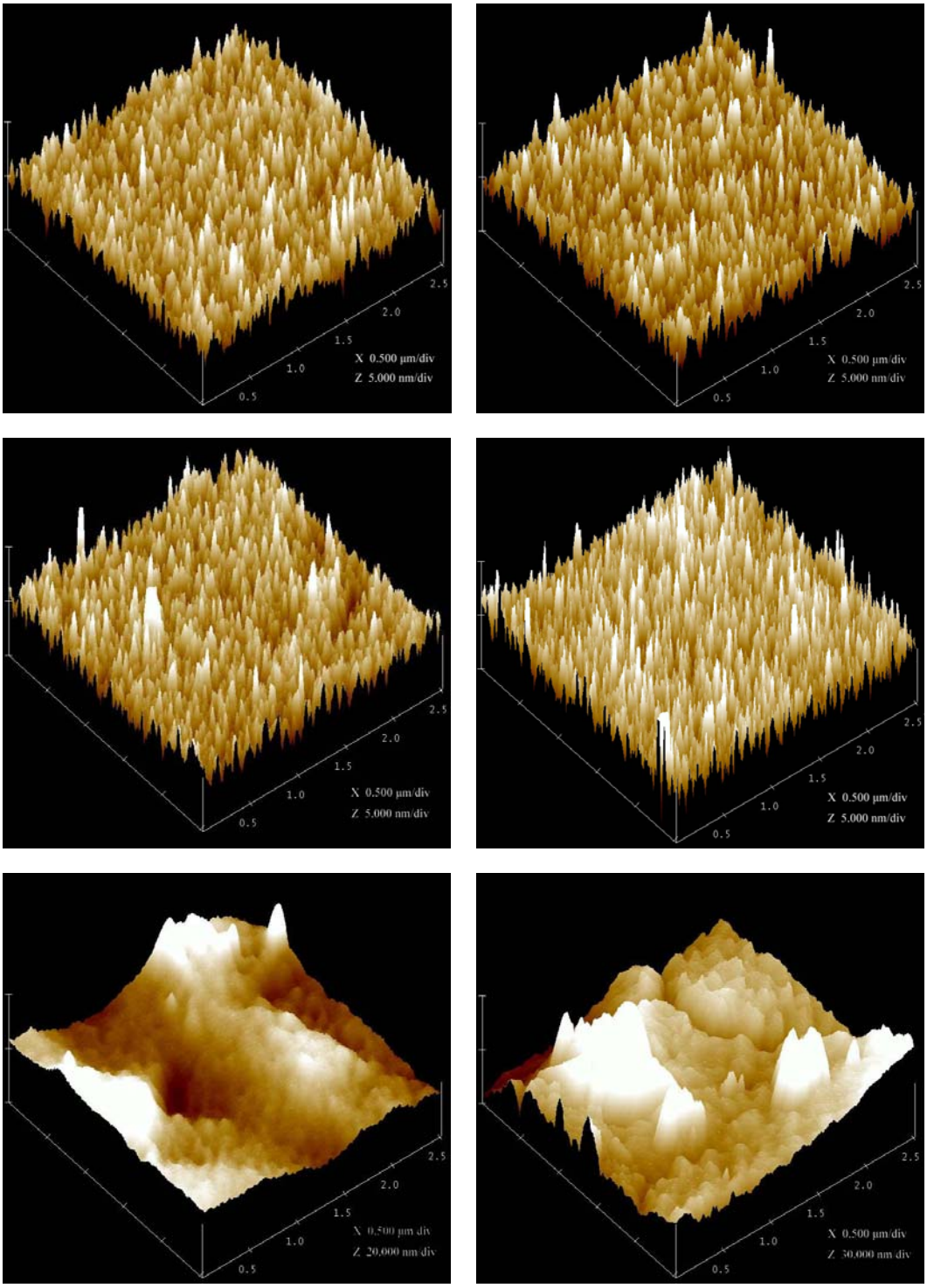

Fig. 5. AFM results of films: (a) as-deposited, (b) 473 K, (c) 673 K, (d) 873 K, (e) 1073 K and (f) 1273 K.

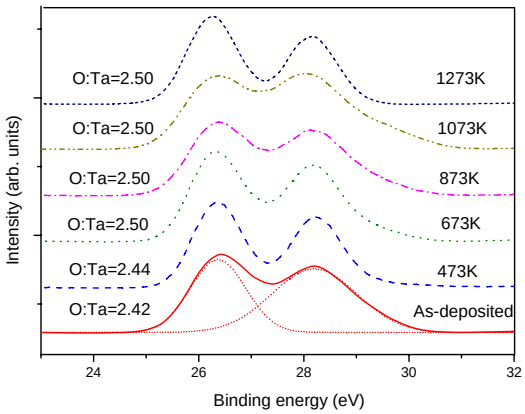

Fig. 6. High resolution XPS spectra of Ta 4f of films.

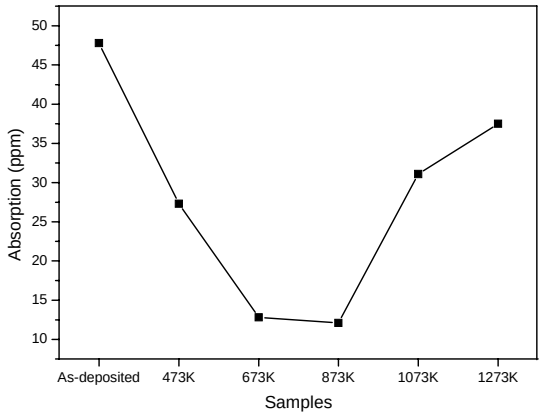

Fig. 7. Absorption of films.

Fig. 7 represents the average absorption data as measured by STL technology. The absorption of films decreases firstly with the annealing temperature increasing and then starts to increase above 1073 K. The minimum absorption is 12.1 ppm when annealed at 873 K. The absorption measured by STL technique is affected by the combination of defects absorption and thermal diffusion of films. When annealed below 873 K, the decrease of absorption is mainly due to the improvement of stoichiometry of films. With the increase of annealing temperature, the O/Ta ratio reaches the theoretical value of 2.50 and the substoichiometric defect disappears, thus the increase of absorption above 873 K is attributed to the reduced thermal diffusion resulted by the appearance of grain boundaries in the crystal growth course. Moreover, as the films annealed below 873 K achieve better stoichiometry and decreased absorption (Figs. 6 and 7), the transmittance is improved. The decrease of transmittance at higher annealing temperature is on account of the increased absorption and scattering loss of grain boundaries.

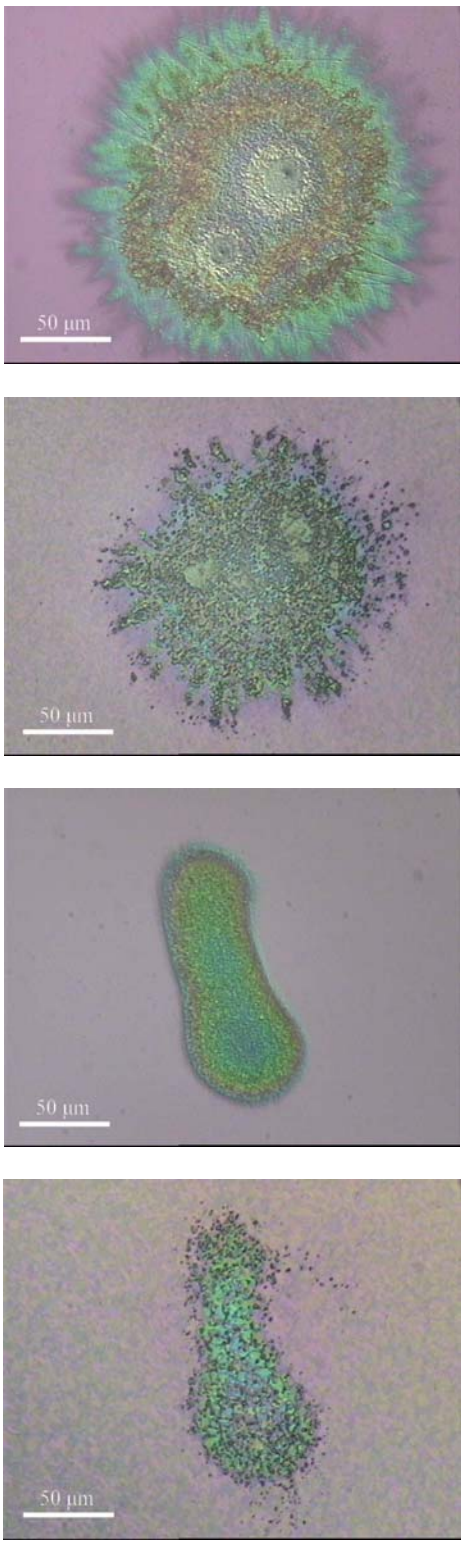

Fig. 8. Typical damage morphologies of films: (a) as-deposited, 1064 nm, (b) 1073 K, 1064 nm, (c) as-deposited, 355 nm and (d) 1073 K, 355 nm.

Fig. 8 shows the typical microscopy images of the damage morphologies at different wavelengths of the as-deposited and 1073 K annealed films. Figure 8(a) displays that some defect points appear in the damaged area, and the damage enlarges from these points. It indicates that at 1064 nm the damage initiates from defects and is consistent with the defect-induced mechanism: as the defect has a larger absorbance index than the film around, it is more liable to absorb laser energy and induce damage. The defect points exist apparently below the annealing temperature of 1073 K. However, the RMS roughness increases significantly above 1073 K and the accidented topography in the surface of films can be observed, thus the defect points are less evident as shown in Fig. 8(b). In addition, some differences are found between the damage morphologies at the two wavelengths. When damaged at 355 nm, Figs. 8(c) and (d) exhibit uniform fused areas without apparent defect points, whereas at 1064 nm there are some defect points in the damage areas.

4. Discussion

The laser damage at the wavelength of 1064 nm always arises by strong absorption points which are induced by defects such as substoichiometry, impurities and imperfect structure [21,22]. Therefore, the characteristic of defects including its kinds and density should be the dominant factor in LIDT of films. The activation energy of substoichiometric defect is only 0.6 eV which is much smaller than the band gap of Ta_2O_5 (4.3 eV), so this defect easily turns into the damage center under laser radiation [23,24]. The O/Ta ratio of the as-deposited film is less than 2.50 as shown in XPS results, indicating that it is substoichiometry. Thus, the damage initiation of the as-deposited film is mainly induced by substoichiometric defect. With increasing the annealing temperature, the substoichiometric defect gradually decreases and it disappears above 673 K. Moreover, during annealing the film structure undergoes a modification and rearrangement driven by the thermal energy. It accompanies with the destruction of unstable bond and the formation of new stable bond, and the decrease of vacancy inside the film. As the annealing temperature increases, the modification effect enhances and the density of structural defect decreases. Therefore, the LIDT improvement below 873 K is due to the reduced substoichiometric and structural defects. The maximum LIDT achieves at 873 K, which can be attributed to the disappearance of substoichiometric defect and the least structural defect. When the annealing temperature increases further, the density of structural defect increases and the thermal diffusion decreases, thus the LIDT of films reduces. The LIDT at 1273 K is lower than that at 1073 K owing to the more grain boundaries and microcracks induced by higher annealing temperature.

However, the damage mechanism at the laser wavelength of 355 nm is different from the above. It is worth noting that the photon energy of 355 nm laser is 3.50 eV near the band gap of Ta_2O_5, so the intrinsic absorption of Ta_2O_5 film will also contribute to the damage initiation. It is illustrated that at 355 nm the reduced substoichiometric defect contributes less to the LIDT (Fig. 1) and the defect points in the damage morphology become less apparent than that at 1064 nm (Fig. 8), indicating that the intrinsic absorption becomes the dominant factor in the damage initiation. Due to the strong affect of intrinsic absorption of the film, the LIDT at 355 nm is much lower than that at 1064 nm. In addition, the LIDT of the films annealed at 1073 and 1273 K decreases significantly and even is lower than the as-deposited film (Fig. 1(b)), which means that at 355 nm the structural defect contributes more to the laser damage than 1064 nm. It is suggested that at shorter wavelength the structural defect with the same size results in larger absorption. The highest LIDT at 355 nm also obtains at 873 K as the defect density is the lowest.

5. Conclusions

Microstructure, optical properties, chemical composition and absorption of Ta_2O_5 films are influenced by wide-range temperature annealing. The correlations of the properties of Ta_2O_5 films during annealing with LIDT at different wavelengths are discussed. It shows that annealing affects the LIDT significantly either at 1064 nm or 355 nm. The damage morphologies show different characters when irradiated at the two wavelengths, indicating different damage mechanism. The LIDT at 1064 nm is mainly influenced by the substoichiometric defect, structural defect and thermal diffusion, whereas at 355 nm it is influenced more significantly by the intrinsic absorption and structural defect.

References

[1] C. R. Wolfe, M. R. Kozlowski, J. H. Campbell, F. Rainer, A. J. Morgan, R. P. Gonzales, Proc. SPIE **509**, 255(1989).
[2] J. -P. Masse, H. Szymanowski, O. Zabeida, A. Amassian, J. E. Klemberg-Sapieha, L. Martinu, Thin Solid Films **515,** 1674(2006).
[3] J. Kolbe, H. Kessler, T. Hofmann, F. Meyer, H. Schink, D. Ristau, Proc. SPIE **1624**, 221(1991).
[4] L. Yuan, Y. A. Zhao, G. Q. Shang, C. R. Wang, H. B. He, J. D. Shao, Z. X. Fan, J. Opt. Soc. Am. B **24**, 538(2007).
[5] H. Krol, L. Gallais, M. Commandré, C. Grèzes-Besset, D. Torricini, G. Lagier, Opt. Eng. **46**, 023402(2007).
[6] D. Milam, W. H. Lowdermilk, F. Rainer, J. E. Swain, C. K. Carniglia, T. T. Hart, Appl. Opt. **21**, 3689(1982).

[7] Y. A. Zhao, Y. J. Wang, H. Gong, J. D. Shao, Z. X. Fan, Appl. Surf. Sci. **210**, 353(2003).
[8] C. Xu, J.Y. Ma, Y.X. Jin, H.B. He, J.D. Shao, Z.X. Fan, Chin. Phys. Lett. **25**, 1321 (2008).
[9] C. Xu, D. W. Li, J. Y. Ma, Y. X. Jin, J. D. Shao, Z. X. Fan, Opt. Laser Technol. **40**, 545 (2008) 9.
[10] C. Xu, Q. L. Xiao, J. Y. Ma, Y. X. Jin, J. D. Shao, Z. X. Fan, Appl. Surf. Sci. (in press).
[11] D. P. Zhang, J. D. Shao, D. W. Zhang, S. H. Fan, T. Y. Tan, Z. X. Fan, Opt. Lett. **29**, 2870 (2004).
[12] Y. A. Zhao, J. D. Shao, H. B. He, Z. X. Fan, Proc. SPIE **5991**, 599117 (2005).
[13] C. Xu, J. K. Yao, J. Y. Ma, Y. X. Jin, J. D. Shao, Chin. Opt. Lett. **5**, 727 (2007).
[14] ISO 11254-1:2000: Lasers and laser-related equipment—determination of laser-induced damage threshold of optical surfaces—Part 1: 1-on-1 test.
[15] J. C. Manifacier, J. Gasiot, J. P. Fillard, J. Phys. E: Sci. Instrum. **9**, 1002 (1976).
[16] Z. L. Wu, P. K. Kuo, Y. S. Lu, S. T. Gu, R. Krupka, Thin Solid Films **290/291**, 271 (1996).
[17] Y. A. Zhao, Y. J. Wang, H. Gong, J. D. Shao, Z. X. Fan, Appl. Surf. Sci. **210**, 353 (2003).
[18] T. Dimitrova, K. Arshak, E. Atanassova, Thin Solid Films **381**, 31 (2001).
[19] J. Gonzalez, M. D. Ruiz, J. B. Rivarola, D. Pasquevich, J. Mater. Sci. **33**, 4173 (1998).
[20] H. Szymanowski, O. Zabeida, J. E. Klemberg-Sapieha, L. Martinu, J. Vac. Sci. Technol. A **23**, 241 (2005).
[21] S. C. Jones, P. Braunlich, R. T. Casper, X. A. Shen, P. Kelly, Opt. Eng. **28**, 1039 (1989).
[22] Y. A. Zhao, W. D. Gao, J. D. Shao, Z. X. Fan, Appl. Surf. Sci. **227**, 275 (2004).
[23] H. Sawada, K. Kawakami, J. Appl. Phys. **86**, 956 (1999).
[24] H. Demiryont, J. R. Sites, K. Geib, Appl. Opt. **24**, 490 (1985).

*Corresponding author: xucheng@cumt.edu.cn.